Wind safety of rubber trees in plantations: methodological analysis of bending experiments on inclined standing trees

Arnauld Clauvy's Engonga Edzang[1, 2]
Benjamin Niez[1]
Lucie Heim[1, 3]
Thierry Fourcaud[4, 5]
Joseph Gril[1, 2]
Bruno Moulia[1]
Éric Badel[1]

[1] Université Clermont Auvergne, INRAE, PIAF
63000 Clermont-Ferrand
France

[2] Université Clermont Auvergne, CNRS, Clermont Auvergne INP, Institut Pascal
63000 Clermont-Ferrand
France

[3] Arts et Métiers Institute of Technology
LABOMAP, HESAM Université
71250 Cluny
France

[4] CIRAD, UMR AMAP
34398 Montpellier
France

[5] AMAP, Univ Montpellier, CIRAD, CNRS, INRAE, IRD
Montpellier
FRANCE

Auteur correspondant / Corresponding author:
Arnauld Clauvy's ENGONGA EDZANG – arnauld.engonga-edzang@inrae.fr

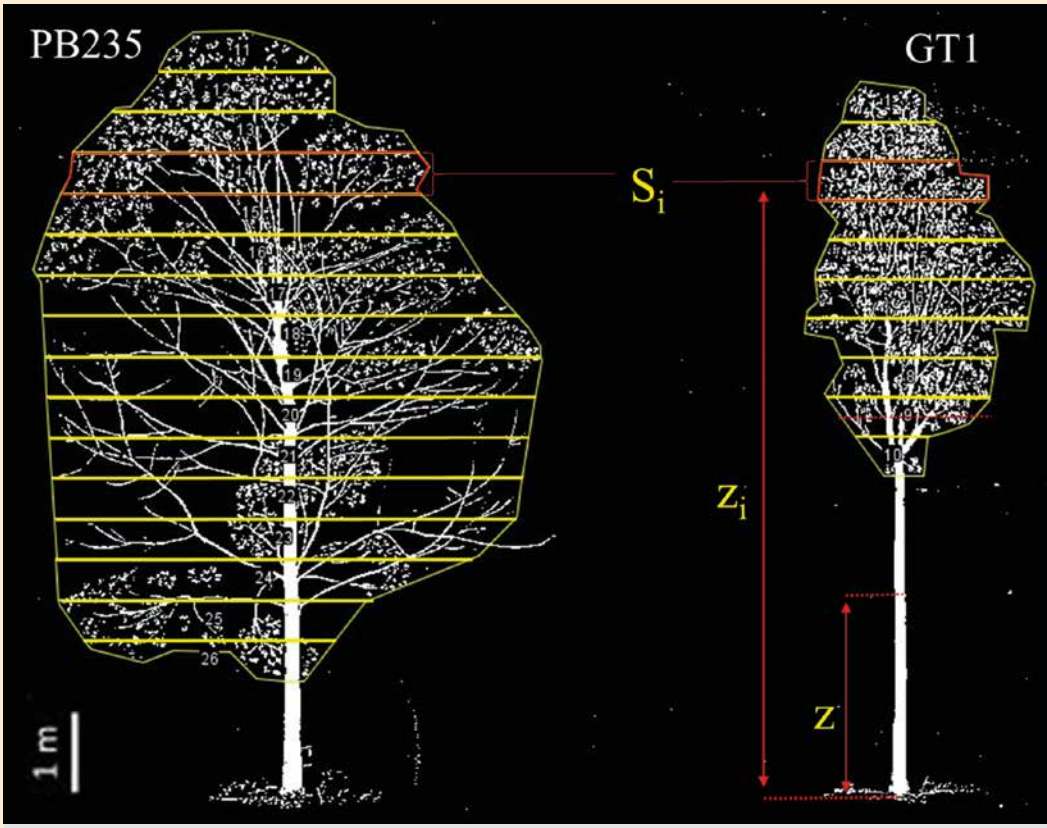

Figure 1.
Drawings of the architecture of two rubber clones (Cilas *et al.*, 2004). PB235 (left) had a height of 9.7 m against 9 m for GT1 (right). After image segmentation, regular subdivisions of the crown surface S are defined for the computation of the bending moment due to the effect of the wind. Each subdivision has the same vertical thickness and its S_i area. Z_i refers to the height of the subdivision.

Doi : 10.19182/bft2022.354.a36912 – Droit d'auteur © 2022, Bois et Forêts des Tropiques – © Cirad – Date de soumission : 9 avril 2022 ; date d'acceptation : 18 août 2022 ; date de publication : 1er décembre 2022.

Licence Creative Commons :
Attribution - 4.0 International.
Attribution-4.0 International (CC BY 4.0)

Citer l'article / To cite the article
Engonga Edzang A. C., Niez B., Heim L., Fourcaud T., Gril J., Moulia B., Badel É., 2022. Wind safety of rubber trees in plantations: methodological analysis of bending experiments on inclined standing trees. Bois et Forêts des Tropiques, 354 : 65-77. Doi : https://doi.org/10.19182/bft2022.354.a36912

Bois et Forêts des Tropiques – ISSN: L-0006-579X
Volume 354 – 4th quarter – December 2022 – p. 65-77
RESEARCH / MECHANICS OF RUBBER TREES IN WIND

RÉSUMÉ

Sécurité des hévéas en plantations face au vent : analyse méthodologique d'expériences de flexion sur des arbres sur pied inclinés

En raison de sa capacité à produire du latex pour des applications industrielles, l'hévéa est cultivé de manière intensive en grandes plantations. Le latex est récolté par saignée de l'écorce, ce qui génère un puits de carbone qui nuit à la croissance secondaire de l'arbre et par conséquent affaiblit la résistance mécanique du tronc. Afin d'étudier la vulnérabilité des clones d'hévéa à la rupture par le vent, nous proposons un modèle mécanique complet qui met en lumière les différents paramètres morphologiques et mécaniques impliqués dans la résistance du tronc en cas de vent fort. Le modèle nécessite des données expérimentales issues de la description structurelle de l'arbre et d'essais de flexion non destructifs réalisés *in situ* dans les plantations. Les résultats permettent d'obtenir une liste des paramètres requis et d'indiquer leur importance relative pour l'estimation du comportement mécanique des hévéas, afin de pouvoir comparer les clones à des fins de sélection.

Mots-clés : hévéa, clone, rupture par le vent, flexion des arbres, Côte d'Ivoire.

ABSTRACT

Wind safety of rubber trees in plantations: methodological analysis of bending experiments on inclined standing trees

Because of their ability to produce latex for industrial applications, rubber trees are grown intensively in large plantations. Latex is harvested by bleeding off the bark, generating a carbon sink for the tree that impairs its secondary growth and consequently weakens the mechanical resistance of the trunk. In order to study the sensitivity of rubber tree clones to wind breakage, we propose a complete mechanical model that sheds light on the different morphological and mechanical parameters involved in trunk resistance to strong wind events. The model requires experimental data that can be recorded from the structural description of a tree and from non-destructive bending tests performed in situ in plantations. The results provide the list of required parameters and indicate their relative importance for estimating the mechanical behaviour of rubber trees, with a view to comparing clones for breeding purposes.

Keywords: rubber tree, clone, wind breakage, tree bending, Côte d'Ivoire.

RESUMEN

Seguridad contra el viento de los árboles de caucho en las plantaciones: análisis metodológico de los experimentos de flexión en árboles inclinados en pie

Debido a su capacidad de producir látex para aplicaciones industriales, los árboles de caucho se cultivan de forma intensiva en extensas plantaciones. La recolección del látex se realiza mediante el sangrado de la corteza, lo que genera un sumidero de carbono para el árbol que perjudica su crecimiento secundario y, en consecuencia, debilita la resistencia mecánica del tronco. Para estudiar la sensibilidad de los clones de árbol de caucho a la rotura por viento, proponemos un modelo mecánico completo que proporciona información sobre los diferentes parámetros morfológicos y mecánicos implicados en la resistencia del tronco a los vientos fuertes. El modelo requiere datos experimentales que se pueden registrar a partir de la descripción estructural de un árbol y de ensayos de flexión no destructivos realizados in situ en las plantaciones. Los resultados proporcionan la lista de parámetros necesarios e indican su importancia relativa para estimar el comportamiento mecánico de los árboles de caucho, con vistas a comparar los clones con fines productivos.

Palabras clave: árbol del caucho, clon, rotura por el viento, flexión del árbol, Costa de Marfil.

Introduction

Rubber tree is the almost exclusive source of natural rubber, which is mainly used by the tire industry, in combination with synthetic rubber, metal, and other ingredients. Cultivated in humid tropical environments, it makes 15 million hectares and produces 13 million tons of rubber per year[1]. Asia alone accounts for 89% of world production, mainly Thailand, Indonesia and Vietnam, while Africa (mainly Ivory Coast) and South America (mainly Brasil and Guatemala) account for 8% and 3% of rubber production, respectively.

Rubber plantations are often monoclonal (Masson and Monteuuis, 2017), with seedling selection based on multiple criteria such as growth speed, tree productivity and its physiological indicators, tapped stand resilience along time, tolerance to abiotic stress such as tapping panel dryness and tolerance to fungus leaf diseases (Gohet *et al.*, 1996; Clément-Demange *et al.*, 2007). However, growers and breeders do not have relevant criteria to estimate the wind breakage sensitivity of trees, and to preventively improve their mechanical resistance.

Indeed, during their economic life in plantation, rubber trees are susceptible to wind damage and especially to trunk breakage (Nicolas, 1979; Fourcaud *et al.*, 1998). However, planters observe a great variability between the different clones. This sensitivity to wind limits the rubber growing areas to regions that do not regularly experience cyclones or typhoons. Even so, wind breakage remains a major issue that reduces the lifespan of the stands and affects farmers' income, with losses in latex production which can get as high as 30% or more in some cases (Clément-Demange *et al.*, 1995). Moreover, two types of wind damage are typically reported by planters in rubber plantations: i) massive tree falls linked to more exceptional events such as big storms, but also ii) regular and local tree breakage under moderate wind storms, which causes continuous annual erosion of the plantation density. The current context of climatic disturbances (Liu *et al.*, 2019; Vecchi *et al.*, 2019) could make the situation even more critical by endangering rubber plantations.

Knowledge of the biomechanical factors and mechanisms related to the breakage of trees because of the wind has greatly progressed during the last decades (Peltola, 2006; Fournier *et al.*, 2013; Gardiner *et al.*, 2016). Experimental and numerical studies allowed disentangling the relative contributions of tree architecture, including the root system, and wood material properties on the biomechanical response to high winds (Sellier and Fourcaud, 2005, 2009; Yang *et al.*, 2017). In particular, the longitudinal distribution of secondary growth along the trunk and the major roots, and the way it is linked to the kinetics of crown development (Bossu *et al.*, 2018) was shown to be a central parameter of trunk breakage sensitivity (Ancelin *et al.*, 2004; Alméras and Fournier, 2009).

To date, several hypotheses have been put forward to explain the sensitivity of rubber clones to wind breakage, including competition between latex production and growth (Watson, 1989; Gohet *et al.*, 1996; Silpi *et al.*, 2006), crown shape (Combe and du Plessix, 1974; Fourcaud *et al.*, 1999; Milet, 2001) or the presence of tension wood (Nicolas, 1979). In tapped rubber trees, the intense and repeated latex production induced by tapping strongly affects the tree's biological activity, particularly the primary and secondary growths. Tapping reduces radial growth of trees by about 50% after only the second week of latex harvesting (Fourcaud *et al.*, 1998), while growth in height is also slightly affected by tapping. Altogether, growth responses result in a decrease of the ratio between radial and height growth. The architecture of the crown is also involved in the trunk breakage phenomena of rubber clones. The shape and branching typology of the crown is very important in windbreak because it contributes to the mechanical moment resulting from wind drag and self-weight (Petty and Swain, 1985), as well as to the structural damping of the tree (Sellier and Fourcaud, 2005, 2009). Considering rubber trees, some clones, known to be susceptible to breakage, are characterized by forked and heavy crown (e.g. RRIM600), or by a continuous growth of the primary axis (e.g. PB235) and in other cases long, heterogeneous and persistent secondary ramifications. In contrast, resistant clones (such as PR107 or PB217) are characterized by i) a balanced crown, ii) a limited growth of the primary axis, and iii) numerous, short, homogenous ramifications, which naturally pruning (Hofmann, 1984; Compagnon, 1986; Milet, 2001). The intrinsic properties of wood formed in trunks were also studied (CIRAD, 1990). The presence of tension wood appears to play an important role in the susceptibility of clones to breakage. This reaction wood, which is anatomically different from "normal" wood, is produced by angiosperm hardwood trees in order to control their orientation, e.g., to keep their straight vertical posture in the face of mechanical stresses (Scurfield, 1973; Donaldson and Singh, 2016). Nicolas (1979) investigated the presence of tension wood in 10 clones and showed that the most sensitive clones to wind breakage were also those that contained the highest proportion of tension wood. Finally, a peculiar morphological feature of most rubber tree clones worldwide is to develop an anemomorphic shape over time, with a tilted trunk and a crown that is curved downwind (Wang *et al.*, 2019). It is not clear whether this trait is adaptive by reducing the wind drag over the tree or detrimental by increasing the overturning moment on the trunk due to the weight of the crown.

In this article, we propose a methodology to evaluate the wind resistance of rubber tree clones with contrasting architectures and having the particularity to grow in an inclined manner. First, a static approach is proposed for studying the wind load over real trees. It is based on the estimation of wind drag forces from image analysis, taking into account tree crown architecture. This information is then integrated in mechanical model equations for a final calculation of the drag force and bending moment.

In a second stage, a simple theoretical model for evaluating the basic mechanical characteristics of standing

[1] https://www.rubberstudy.org/

Bois et Forêts des Tropiques – ISSN: L-0006-579X
Volume 354 – 4th quarter – December 2022 – p. 65-77

rubber clones is presented. It can be used to estimate the bending stiffness of the trunk and the modulus of elasticity of its wood, as well as the maximal bending stress in the trunk (related to its risk of breakage).

The parameters required for this model can be estimated using a controlled bending test that can be performed in situ in the plantation. In this case, the static load (bending moment) differs from the load induced by wind drag and is modelled from simple measurements.

Finally, the maximal bending stress that occurs in the trunk of the tree for a typical wind storm can be calculated (as this is the trait that may trigger stem breakage), and different clones can be compared for their level of mechanical stress during wind storm. Besides, if the strength of wood is known, then the safety factor of each tree form trunk breakage can be estimated.

A practical application was performed using data provided from previous pulling tests carried out in 1997 on two rubber tree clones in Ivory Coast plantations. These two clones were selected because of their contrasted mechanical sensitivity to wind breakage during strong windy events: the PB235 clone is known as very susceptible to wind breakage, whereas GT1 clone is considered as more resistant to wind breakage, at least in the young age (Obouayeba *et al.*, 2012).

The objective of this case study is to give an overview of the mechanical information that can be extracted from such experimental data. We highlight all the parameters that are necessary for data analysis, even if the small number of experimental tests performed and the absence of some data did not allow to provide a robust statistical analysis and are principally described for illustrative purpose. Finally, the importance of crown weight and of tree tilt and crown curvature in the calculation of the bending moment is discussed.

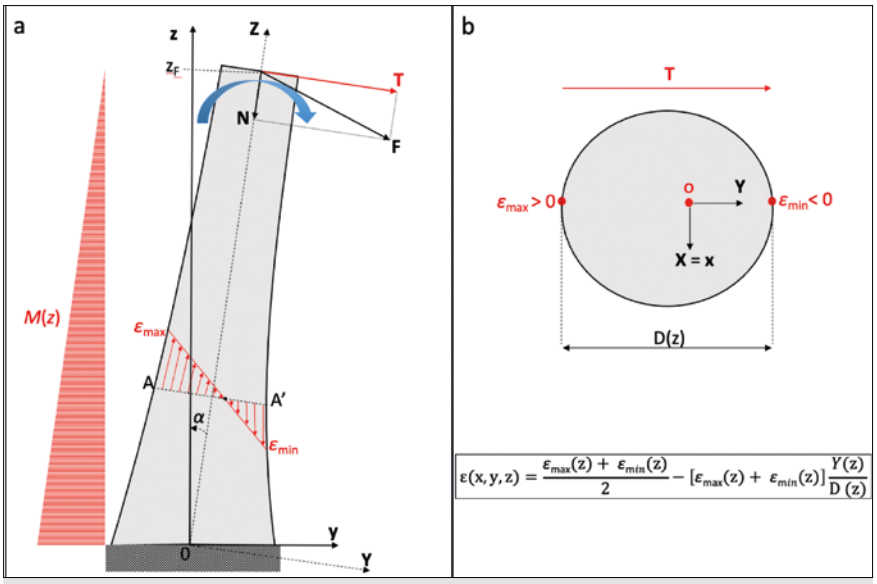

Figure 2.
Simplified mechanical model of a tree trunk under externally applied bending: a. Longitudinal section of a trunk. b. Circular cross-section (A-A') of the trunk. The loading results from a force F applied at point z_F and have two components: the force N that is normal to the cross section and the shear force T (red arrow). T generates a bending moment *M*(z) (red hatched triangle) that induces a rotation of the cross-sections and a local mechanical field of longitudinal deformations ε(x,y,z) in the cross section. The initial inclination of the tree at the base is *α*. For a given altitude z, the longitudinal strain varies linearly from the pith (ε = 0) to the periphery of the trunk where the strain is maximal (for y = D/2).

Material and methods

Estimation of the wind drag force and the wind-induced bending moment in the trunk by image analysis

The analysis of the tree's behaviour in the wind requires knowledge of the action of the wind on the tree, i.e., the drag force. The aim of this section is to present a method to evaluate this action on the studied trees. The method is based on a scaled description of the crown morphology and the knowledge of a theoretical wind profile. The crown morphology can be obtained using representative photographs. But it can be also obtained by accurate drawings. This is the case illustrated in figure 1 using published drawing representing the two rubber clones, PB235 and GT1, by Cilas *et al.* (2004). The method presented here aims at comparing the drag force and the resulting bending moment that the trees could experience for the same given wind profile.

The method follows five main steps (figure 1):

- First, the initial drawing is converted into an 8 bit-grey image and segmented in order to get a binary image that distinguishes the tree structure (branches, leaves) from the porosity.
- The boundary of the tree crown is drawn. This defines the total crown area S, perpendicular to the wind direction.
- This surface S is then divided into n horizontal slices, 50 centimeters thick each. The number n of slices depends on the total thickness of the crown (figure 1).
- For each slice, the area Si, leaf density di and the height zi of the centre of mass are measured. The leaf density di is computed as the percentage of the area corresponding to non-null pixels i.e. white pixels. So that, di.Si stands for the effective area of the slice.

In the case of a given wind profile U(z), the local force Fi applied by the wind on each slice is estimated as:

$$F_i = \left(\frac{1}{2}\right) \rho_{air} U_i^2 c_d d_i S_i \text{ with } i \in [\![1;n]\!] \qquad (1)$$

where $U_i = U(z_i)$ stands for the local wind velocity ($m.s^{-1}$), ρ_{air} the air density and c_d is the drag coefficient we fixed at 0.2 in the following calculations, as indicated to Stuttgart table (Brudi et van Wassenaer, 2002).

Finally, the local bending moment M_i due to the interception of the wind by each of these subdivisions S_i is computed as:

$$M_i(z) = F_i (z_i - z) \text{ with } i \in [\![1;n]\!] \qquad (2)$$

where z is the critical point of interest of the trunk (trunk collar for instance, $z = 0$) where the bending moment is analysed. The total bending moment $M(z)$ induced by the drag forces and applied to the trunk of the tree is computed as the sum of these local bending moments M_i:

$$M(z) = \sum_{i \in [\![1;n]\!]} M_i(z) \qquad (3)$$

The above-mentioned computation was performed using ImageJ software (figure 1).

Note that this wind-drag model neglects the crown reconfigurations that occurs when the crown is submitted to high winds (Gardiner *et al.*, 2016). These reconfigurations reduce the front area of the crown S as well as the drag coefficient c_d (through branch streamlining). However, we have no data for this for rubber trees in plantations. Nevertheless, the estimate of the bending moment given by equation (3) can be considered as an upper-bound estimate, which makes sense in the view of assessing wind firmness and plantation security.

Once the bending moment along the trunk resulting from wind drag over the crown has been obtained, the next step is two estimate the flexural rigidity of the trunk and the stress that bending can create. This can be achieved through a theoretical bending model.

Modelling of trunk bending

The following model is primarily designed to analyse a pulling test used to estimate the bending rigidity of the trunk, but will also lead to a stress analysis applicable to the effect of wind. The tree stem is described as a straight, near-vertical beam embedded at its basis and free to move at its top (figure 2a). The cross section is assumed to be circular along the length of the beam with a decreasing diameter $D(z)$ (figure 2b).

Rubber trees in plantations often show a small initial deviation from verticality that is due to the direction of dominant wind. This inclination is characterized by the angle α between the direction of the trunk Z and the vertical direction z (figure 2). A load F is applied at height z_F on the trunk. The force is applied in the plane (y,z), either in the direction of the initial inclination α or opposite to it, and its direction makes the angle β with the horizontal direction. The cross section situated at height z < zF is subjected to a normal load N and a bending moment M given by:

$$N = F \cdot \sin(\beta - \alpha) \quad ; \quad M = F \cdot \cos(\beta - \alpha) \cdot [z_F - z] \,/\, \cos\alpha \qquad (4)$$

According to Euler-Bernoulli's theory for slender beams, the distribution of axial strain ε within the cross section is a linear function of the position Y relative to the plane (x,Z):

$$\varepsilon = \delta\varepsilon - \Delta\varepsilon.(2Y/D) \qquad (5)$$

where $\delta\varepsilon$ is the average strain and $\Delta\varepsilon$ the differential strain between the inner and outer sides of the trunk. At mechanical equilibrium, and assuming a cross-section made of an homogeneous elastic material of Young's modulus E, $\delta\varepsilon$ and $\Delta\varepsilon$ can be related to the normal load N and the bending moment M through the following relationships:

$$\delta\varepsilon = N \,/\, (E.S)$$
$$\Delta\varepsilon = M.D \,/\, (E.J)$$
$$E = M.D \,/\, (J.\Delta\varepsilon) \qquad (6)$$

$S = \pi D^2/4$ being the surface area of the circular cross section and $J = \pi D^4/64$ its second moment of area. From equation (4) and (6) the ratio $\delta\varepsilon/\Delta\varepsilon$ can be derived:

$$\delta\varepsilon \,/\, \Delta\varepsilon = [D \,/\, (z_F - z)] \cdot \tan(\beta - \alpha) \cdot \cos\alpha \,/\, 64 \qquad (7)$$

showing that, except for an anchoring position close to the tree collar (small β-α) or a cross section close to the force application point (zF - z < D), δε can be neglected and ε varies from -Δε/2 on the compressive face (Y = +D/2) to +Δε/2 on the tensile face (Y = -D/2). Then, the peripheral longitudinal stress, given by -σ and +σ, respectively, comes as:

$$\sigma = M.D \,/\, (2.J) \qquad (8)$$

Note that equation (8) would also apply to the case of a wind-induced bending moment M such as given by equation (3). In both cases the mechanical stress σ can be compared to the breaking stress (material strength) σ_r, leading to wood rupture estimated for these genotypes and which can be estimated by conducting a bending test up to stem rupture or by direct assessment on (green) wood sample using a testing machine. The safety factor (SF) comes as:

$$SF = \sigma_r \,/\, \sigma \qquad (9)$$

SF characterizes the wind firmness; the higher is SF, the safer the tree with respect to its trunk. As a remark, these estimations of σ and σ_r do not take into account the nonlinear response that precedes failure. In the case of σ_r, the pre-existing growth stress distribution should be also taken into account, especially in the case of tension wood occurrence (Gril *et al.*, 2017).

Field experiments: Bending of standing trees

Plant material

The tests were carried out in Ivory Coast, in the experimental part of the Anguededou rubber tree plantation depending on the CNRA research center of Bimbresso, near the road from Abidjan to Dabou (5°18'53.3"N 4°09'19.8'W). In this location, the soils are made of very deep tertiary sand, which makes possible a deep growth of the tap-roots of the trees, and therefore very little uprooting by wind. Wind damage is here predominantly the result of trunk breakage.

Nine rubber trees were selected in 3 different plots: 5 trees of the PB 235 clone and 4 trees of the GT1 clone; 3 trees were tapped for 2 years, and 6 trees for 5 years. The trees were 7 to 11 years old and were selected from 4 different plots. The diameter of trees at 1.30 m height ranged from 16.2 to 24.2 cm, i.e. from 51 to 76 cm in girth (table I). The total height varied in the range 20-25 m. The height of insertion on the trunk of the lowest branch was around 8 m. The initial inclination of the trees was about 1 to 7° (table I) in the direction of prevailing winds.

Bois et Forêts des Tropiques – ISSN: L-0006-579X
Volume 354 – 4th quarter – December 2022 – p. 65-77

Table I.
Characteristics of the different tested trees. The trees were 7 or 11 years old, had 2 or 5 years of tapping, and an initial inclination of 1 to 7° in the direction of the prevailing wind.

Tree number	Clone	Plot	Age	Nb tapped years	Diameter at 1.3 m (cm)	Initial inclination (°)	Trunk weight (kg)	Branch + leaf weight (kg)
1	PB235	1	11	5	17.5	5.3	153.0	180.5
2	PB235	1	11	5	17.7	3.4	173.6	177.9
3	PB235	2	7	2	20.7	1.3	257.6	228.5
4	PB235	2	7	2	16.6	3.0	194.2	106.5
5	PB235	1	11	5	24.2	3.6		
6	GT1	2	7	2	16.2	4.8	104.0	125.5
7	GT1	3	11	5	20.5	2.9		
8	GT1	3	11	5	23.6	3.2		
9	GT1	3	11	5	17.5	3.1		

Experimental design of the in situ bending test

Bending tests were carried out between 10 and 30 July 1997. These tests aimed at characterizing and comparing the mechanical response to bending of PB235 and GT1 clones. The total height of the tree H, the height $H_F = z_F$ at the point of attachment of the cable to the trunk, the initial inclination of the trunk α and the angle of the cable with the horizontal β, the distance from the trunk to the point of attachment of the tree L_{hw} were measured before the bending experiments (cf. figure 3). In addition, girth was recorded at different heights: first at 0.3 m height and then every 1 m up to the height of application of the force.

Strain sensors were installed at five different heights along the stem (0.3, 1.3, 2.3, 3.3, 4.3 m). For each height, one sensor was fixed on the part of the trunk under compression and a second was fixed on the part under tension. The design of the strain sensor (figure 4) was inspired by the sensors developed by Blackburn (1997) and described in Moore *et al.* (2005). The contraction (resp. stretching out) of the wood fibres generates a length variation between two lever arms, which generates the bending of the thin central part of the sensor. A strain gauge was glued on this thin zone to evaluate the corresponding bending. A second gauge was fixed to the sensor to provide temperature compensation without being subjected to mechanical strains (figure 4).

The force applied during loading was measured using a dynamometer with a maximum capacity of 10 kN. During the experiments, a hand winch was used to pull the tree. The transducers data and the length of the cable pulled were recorded at each loading step. All trees were pulled both in the direction of the natural inclination and opposite to it. For trees n° 1, 2, 6, and 9 (two trees per clone), the test was then repeated along the inclination and brought up to tree failure. The failure force and the failure height of the tree were noted at the end of the bending test. For the trees n° 1, 2, 3, 4 and 6 (table I), after each bending test, the trees were felled and split into three parts: trunk, branches and leaves. Each part was individually weighed.

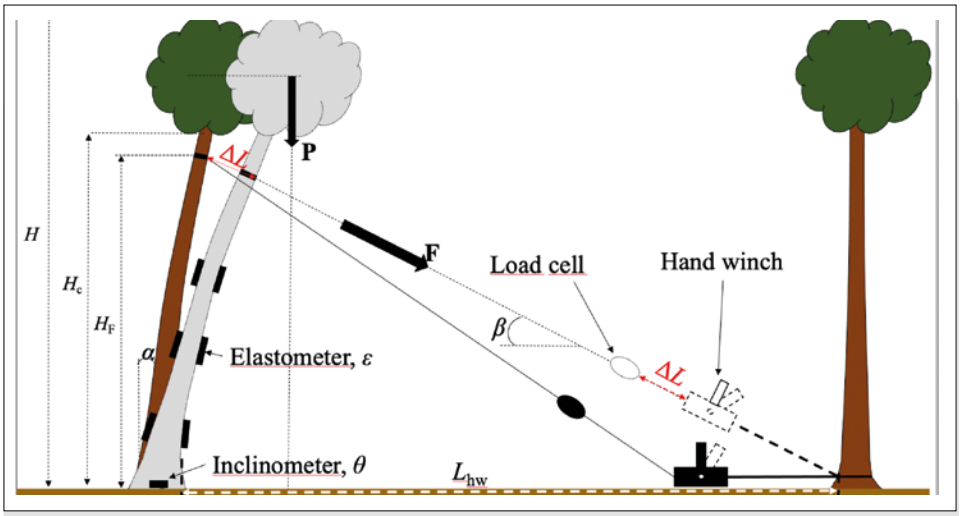

Figure 3.
Principle of a trunk-bending test. H: total height of the tree. Hc: height of crown base. HF = zF: height at wire rope fixation point on the tree. α: initial tree inclination tree at the base. β: angle of cable with the horizontal. Lhw: distance from the tree to the anchoring point of the hand winch at base of neighbouring tree. ε: strain measured by the elastometer. θ: inclination of root-soil system measured by the inclinometer. F: force applied by the hand winch. P: crown weight. ΔL: shortening of cable length.

Estimation of the bending moment on the trunk during the bending tests

Mechanical analyses of pulling tests were carried out using recorded data (i.e. incremental strains, inclination angles, etc.) in the theoretical model described above. The bending moment M was computed at the location of strain gages and each pulling step using equation (4b), the longitudinal Young's modulus E was obtained using equation (6), and the bending stiffness was defined as the product $E.J$. Using these parameters, the theoretical model of stem bending can now be coupled with the model for estimating wind drag in storm conditions and the resulting bending moment. Then the maximal stress under such winds can be estimated and compared between clones.

Results and discussion

Estimation of the drag forces and the resulting bending moment

The vertical profile of wind speed $U(z)$ depends on the roughness of the canopy and can be experimentally measured in situ. Since we lacked such experimental data, we chose a realistic model depicted in the literature. Data and models of the wind vertical profile in the specific case of rubber tree plantation are lacking. Moreover, their extrapolation from wind models in forests is not straightforward, because the rubber tree plantation is less dense. Therefore we considered the situation where the static wind load on the tree is maximal, that is when the tree is sitting on the canopy edge facing a clear lad surface winward (e.g. when the upwind plot has been clear-cut). In such case with an upwind surface with a roughness near zero, the wind profile can be modelled as a logarithmic curve (Gardiner *et al.*, 2016):

$$U(z) = \frac{U_{10}}{\ln(z_0 * K)} * \ln(z) \qquad (10)$$

where U_{10} is equal to 33,3 $m.s^{-1}$, namely 120 $km.h^{-1}$, and stands for the velocity of wind of grade 12 on the Beaufort scale (higher grade). This velocity is assumed to be measured at 10 m high as indicated in the Eurocode 1-part 4 for the velocities of the reference wind on opened fields. K is the Von Karman constant and z_0 stands for the length of roughness and is assumed equal to 0.01 m (Cook, 2007; Gardiner *et al.*, 2016).

Using these windy conditions, we used equations 1 to 3 to evaluate the drag force at each height and the resulting bending moment applied to the trunk. We computed this bending moment for both clones by taking into account their specific architecture, shown in figure 1. As can be seen, PB235 and GT1 clones displayed almost identical heights (9.7 m for PB235 and 9 m for GT1), but very different crown sizes and shape. Overall, the front area of the crown of PB235 was 4.2 times higher than that of GT1 (39.5 m^2 vs 9.5 m^2). The computations showed that the bending moment at the trunk basis (1-meter-high) of the PB235 clone was 72% higher than for the GT1, with values of 271 N.m and 464 N.m, respectively. This is substantially higher but far less than the difference in the front area. This is because GT1 had a narrower crown that was gathered in its upper part (where wind drag is higher and lever arms are maximal) while PB235 had a wider crown but more evenly distributed over its height.

Mechanical behaviour of rubber tree trunks

The results presented in table II were computed thanks to the strain measurement performed at 1.3 m high and all the equations described in the previous section for clones PB235 and GT1. The values in brackets in the fourth column of the table correspond to the average value of the five moduli calculated from the deformation measurements over the five heights (0.3, 1.3, 2.3, 3.3 and 4.3 m). The low number of fully documented experimental tests did not allow for providing a robust statistical analysis. However, a few parameters can be discussed. First, the mechanical tests enlightened a slightly (but significant) higher bending rigidity for the PB235 clone. Theoretically, this parameter is the combination of the dimensions of the cross-section and the Young's modulus of the wood material. In our case, the analysis of the strain vs force curves indicated a large difference in term of Young's modulus: PB235 showed a higher average elastic modulus (+ 31%) than GT1 with values equal to 7.4 GPa and 5.1 GPa respectively.

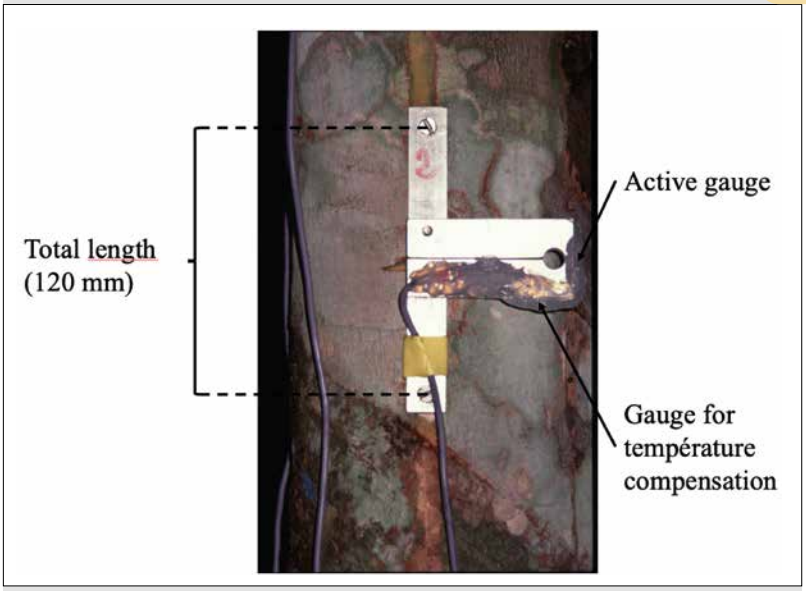

Figure 4.
Strain sensor screwed in the wood during the bending tests of the trunk (© T. Fourcaud).

Comparison of the wind susceptibility of the two rubber tree clones

The two clones were selected based on their known contrasting sensitivity to wind. While both clones had the same age and trunk diameter, the full analysis of the experimental data, coupled with mechanical modelling, revealed a strong difference in longitudinal elastic modulus between the clones. PB235 had a much higher Young's modulus (p-value = 0.012), which resulted in higher bending stiffness of the trunk and thus lower stem deformations for a given force. However, the wider crown of the PB235 drastically increased the area of wind interception, the drag force and the resulting bending moment applied to the trunk. Based on these results, we were able to estimate the maximum stress that the trunk could be subjected to under the wind conditions described in Section 2.1. The calculations indicated that the maximum stress induced by the wind drag was higher for PB235 than for GT1 (0.69 MPa for PB235 and

Table II.
Results of bending tests for PB235 and GT1 rubber clones. The values in brackets for the MOE correspond to the average value of the five moduli calculated from the deformation measurements over the five heights. The failure stress is estimated according to equation 8. Empty cells indicate missing data. Stars indicate the statistical difference between PB235 and GT1 clones. (*: p < 0.05) (Student T-test).

Tree number	Clone	Bending rigidity, *EJ* (kN/m²) *	Average MOE, *E* (GPa) *	Failure force (kN)	Bending moment at failure, *M* (kN/m)	Failure stress at 1.3 m, σ_{max} (MPa)	Failure height (m)
1	PB235	359.7	7.8	5.69	22.08	41.92	1.3
2	PB235	368.2	7.7	4.71	18.06	33.37	0.71
5	PB235	638.7	7.1				
7	PB235	265.3	7.2				
8	PB235	907.9	5.4				
6	GT1			5.30	20.47	48.73	1
9	GT1	505.9	5.8				
10	GT1	725.3	4.8				
11	GT1	244.4	5.3	5.89	22.74	43.17	1.6
Mean PB235		507.9	7.0	5.2	20.1	37.6	1.0
Standard deviation PB235		263.4	1.0	0.7	2.8	6.0	0.4
Mean GT1		491.9	5.3	5.6	21.6	46.0	1.3
Standard deviation GT1		240.8	0.5	0.4	1.6	3.9	0.4

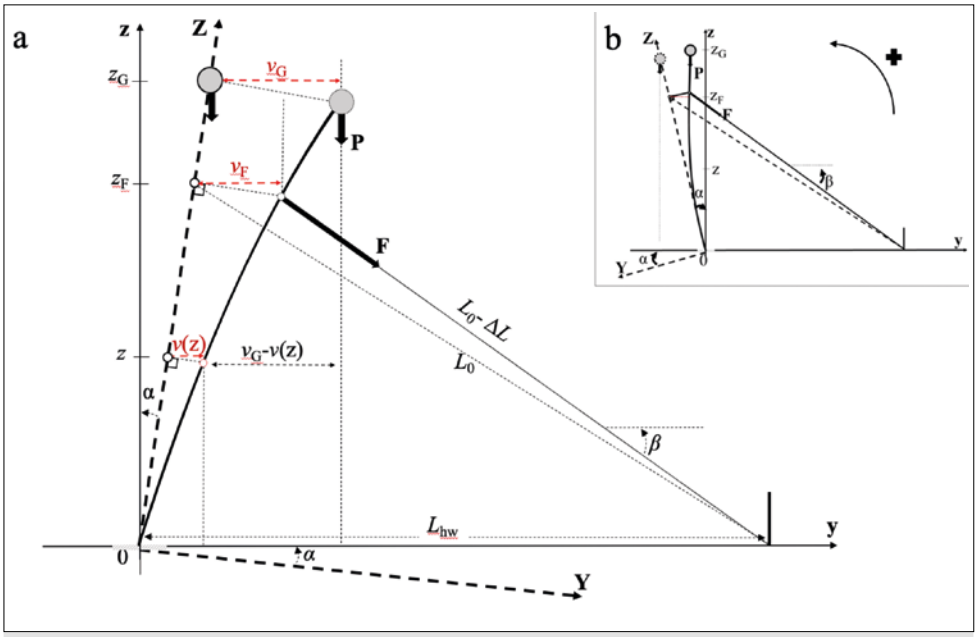

Figure 5.
Diagram of the bending test on standing tree. a. Bending in the direction of natural inclination of the tree. b. Bending in the opposite direction to natural inclination of tree. L_0: initial length of tensioned bending cable, (O, y, z) fixed reference frame and (O, Y, Z) rotating reference frame related to the tree inclination. *v*(z): displacement of tree at position *z* in the (y,z) plane. v_F: displacement of the point of force application. v_G: displacement of the gravity centre of the crown. z_F: position of the point of force application. z_G: position of the gravity centre of the crown. α: initial inclination of the tree at the base. *β*: angle of cable with the horizontal. L_{hw}: distance from the tree to the anchoring point of the hand winch at base of neighbouring tree.

0.4 MPa for GT1) for a similar trunk diameter of about 19 cm.

These values can be compared to the breaking stress (wood strength) leading to wood rupture at 1.3 m height estimated for these genotypes: σ_r (42 MPa for PB235, 46 MPa for GT1). This would lead to high safety factors *SF* against a grade 12 wind storm (120 km/h), *SF* = 61 for PB235 and *SF* = 114 for GT1, with GT1 being almost 2 times safer. However, these values have just an illustrative purpose: indeed, the values for wood strength σ_r were obtained for 1 or 2 trees per genotypes and the wind-drag estimation comes from mean crown shapes from another experiment (although from the same pedoclimatic area).

Consequently, it is essential to perform both analyses to correctly estimate the wind resistance of the trees: wind profile and tree crown architecture to determine the wind loads and the bending moment applied to the trunk; evaluation of wood mechanical behaviour through controlled bending tests and finally computation of safety factors.

Estimation of the bending moment with consideration of the crown weight

The expression of *M* given by equation 4b is only valid for small perturbations of the system, characterized by small levels of *v*(z), displacement of the cross-section along y-direction at height *z*. As soon as the trunk is significantly bent, additional contributions to *M* result from the modified geometry. In the case of wind loading, Ancelin *et al.* (2004) reported the impact of crown weight when the trunk bends. In the case of a standing tree bending test, Langbour (1989) proposed a model based on a direct but complex calculation. We propose here a simplified model based on the measurement of the cable shortening for the estimation of the effect of the crown weight. First, the normal component *N* contributes by

$\delta M_N = N\,[v_F - v(z)] / \cos\alpha$ where $v_F = v(z_F)$. Second, due to the movement of the part of the tree supported by the cross section, its weight $P(z)$ contributes by $\delta M_P = P(z)\,[v(z_G) - v(z)]$ where G(z) is its gravity center, z_G the height of G(z) and $v(z_G)$ is its horizontal movement. For the determination of the position z_G, we assume that the masses of the different branches are distributed along the axis of the trunk and that they are added to the local mass of the trunk. Thus, using the masses of the different parts of the trunk and the masses of the different branches and their positions, we determine the position z_G from the following equation:

$$z_G = z_F + \sum_{z_i>z} gm_i \cdot z_i \;/\; \sum gm_i \qquad (11)$$

The total bending moment M supported by the cross section becomes:

$$M = M_T + \delta M_N + \delta M_P \qquad (12)$$

$$M = F.\cos(\beta-\alpha)\cdot[z_F - z] / \cos\alpha + F.\sin(\beta-\alpha)\cdot[v_F - v(z)] / \cos\alpha + P\cdot[v(z_G) - v(z)]$$

where M_T is the main component of the bending moment given by the equation 4b. Since $v(z)$ depends on F, this formulation is implicit and its rigorous resolution is complex. However, δM_N and δM_P being second-order corrections, they can be approximated using a simplified tree model. If the trunk was homogeneous and perfectly cylindrical up to the force application point, and the upper part of the tree made of a weightless and rigid bar holding the concentrated weight $P(z)$ at point G(z) (as shown in figure 5), the expression of $v(z)$ could be simply written as:

$$v(z) = v_F\cdot[2 - (3/2)\cdot(z/z_F)2 + (1/2)\cdot(z/z_F)3] \quad \text{for } 0 < z < z_F \qquad (13)$$

$$v(z) = v_F\cdot(3/2)\cdot(z - z_F)/z_F \quad \text{for } z_F < z \qquad (14)$$

This bending model does not take into account the deformation of the stem above the force application point, nor the reconfiguration of the crown. The displacement v_F can be obtained independently based on the variation of the rope length $\Delta L = L\text{-}L_0$ and of the rope angle $\Delta\beta = \beta - \beta_0$ where L_0 and β_0 are the initial value of rope length L and rope angle β, respectively (figure 5). Assuming small values of $\Delta\beta$ and $\Delta L/L_0$, and replacing $L_0 = z_F/\sin\beta_0$, we can write:

$$L_{hw} - z_F\cdot\tan\alpha = L_0\cdot\cos\beta_0 = v_F + (L_0 + \Delta L)\cdot\cos(\beta_0 + \Delta\beta)$$

$$\sim v_F + L_0.\cos\beta_0 + \Delta L\cdot\cos\beta_0 - z_F\cdot\Delta\beta \qquad (15)$$

$$\Rightarrow v_F \sim -\Delta L\cdot\cos\beta 0 + z_F\cdot\Delta\beta$$

The estimation of $P(z)$ and $z_{G(z)}$ requires values of weight, dimensions and rough positioning of tree portions, that can be measured after tree felling. Based on such data, and using the relative horizontal displacement $v(z)/v_F$ and v_G/v_F provided by equations 13 and 14, the total bending moment M can be calculated, and the local bending rigidity $E.J$ or Young's modulus E, at the level of the cross-section z, derived from equation 6:

$$E.J = M.D \;/\; \Delta\varepsilon \qquad (16)$$

$$E = M.D \;/\; (J.\Delta\varepsilon) \qquad (17)$$

Note that in case of a bending test performed in the direction opposite to the initial natural inclination of the trunk, the previous equations (15) and (16) remain applicable, with a negative α value (figure 5b).

This complete analysis could be applied in the case of one single bending experiment (tree 1, table I), where all the parameters needed were available. The objective here is to evaluate the contributions of the vertical component of the force F (δM_N) and of the weight of the tree crown P (δM_P), often neglected, to that of the horizontal component of the force F (M_T) according to the equation 11. For this, in addition to the data of force evolution F, rope shortening ΔL and rope angle β, we needed geometrical parameters such as: tree height, height at the base of the tree crown, height of the cable on the tree, distance from the tree to the anchor point of the lag bolt, natural inclination of the tree. We also need the mass of the trunk, the mass of the branches and the girth at different heights for the calculation of the position of the centre of mass.

The histograms in figure 6 present the proportions of M_T, M_N, and M_P in the total moment M for different height levels (0.3, 1.3, 2.3, 3.3, and 4.3 m), in cases of bending in the direction of the natural inclination (NI) and in the direction opposite to the natural inclination (ONI). In case of NI bending, M_T represented more than 80% of the total moment M between heights 0.3 m and 1.3 m, while δM_N and δM_P contributed by only 2% and 18% to the total moment M, respectively, for the same height levels. Above 1.3 m, the relative influence of M_T decreased progressively (about 52% of M at 4.3 m) at the expense of δM_P that reached about 46% of the total bending moment M at 4.3 m. In case of ONI bending, the proportions of M_T, δM_N, and δM_P were different. M_T represented only 70% of M between 0.3 and 1.3 m while δM_N and δM_P represented respectively 8% and 20% of M for the same height levels. Above 1.3 m, as, for NI bending, the proportion of M_T decreased considerably (only 44% of total M at 4.3 m) while the influence of δM_P increased (50% of total M at 4.3 m). The relative influence of δM_N remained low and almost stable with height in both bending cases. Between 0.3 and 4.3 m, the influence of δM_N decreased from only 1.7 % to 1.5% for NI bending and from 8% to 6% for ONI bending.

In conclusion, the closer to force application point, the higher is the relative influence of δM_P in the total bending moment M. The error generated by neglecting the effect of the weight was very significant for the highest altitudes. This can simply be explained by the decrease of M_T that became zero at the force application point. Comparatively, the error due to neglecting the contribution of δM_N remained low in all cases although not negligible; it can be taken into account to improve the quality of the analysis. This confirms the analysis of Papesch *et al.* (1997) who already highlighted the role of the crown weight.

The M/M_T ratio can be used to determine a correction factor to M_T for each height, when the bending moment has been calculated with a conventional beam analysis. The variations of M/M_T ratio are shown in figure 7 as a function of

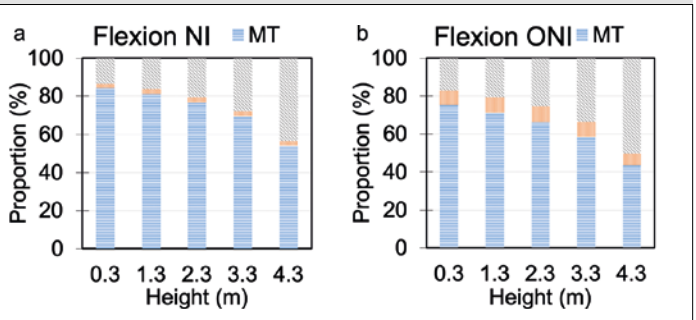

Figure 6.
Relative contribution of the three terms of equation 11 (MT, δMN and δMP) to the total moment M at different heights (0.3, 1.3, 2.3, 3.3, and 4.3 m). The force intensity was F = 2.7 kN and was applied at zF = 5.3m. a. Case of bending in the direction of the natural inclination (NI) of the tree. b. Case of bending in the opposite direction of the natural inclination (ONI) of the tree. MT is the moment due to the horizontal component of the force. δMN is the contribution of the vertical component of the force. δMP is the contribution of the weight of tree crown.

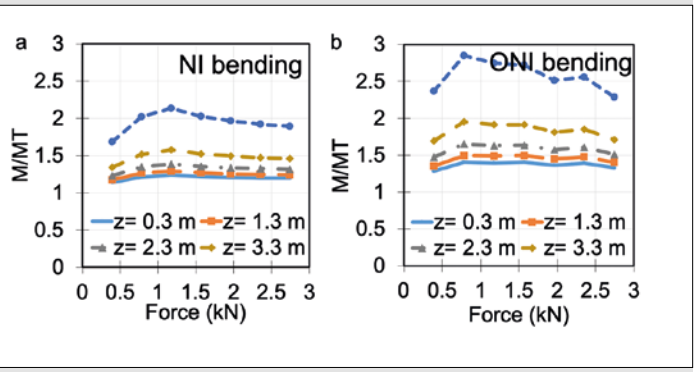

Figure 7.
Evolution of the M/M_T ratio as a function of the force. a. Case of bending in the direction of the natural inclination (NI) of the tree. b. Case of bending in the opposite direction to the natural inclination (ONI) of the tree. Computations were performed for 0.3, 1.3, 2.3, 3.3 and 4.3 m heights. *M* represents the total bending moment. M_T is the bending moment due only to the horizontal component of the force F.

the applied force F, for NI or ONI bending. As expected, in both cases M/M_T increased with the height. It was higher in case of ONI bending (figure 7b) compared to NI bending (figure 7a). For a given height, this M/M_T ratio remained almost constant as the force increased, suggesting that a simple function of height could be taken as a correction factor to M_T moment.

The above reasoning could also be achieved when the bending is due to wind drag instead of artificial pulling. In this case, for example at 1.3 m height within the trunk, the actual stresses could be increased by 20% on the tree 1 of PB235. It is not possible however to pursue this line of reasoning on the available test example because we lack data for GT1 and have no repetition.

Required data for a full mechanical analysis

In the context of the rubber tree plantation, we enlightened the essential parameters required to undertake an estimation of the tree resistance to wind. For this, we designed a novel theoretical mechanical modelling that takes into account all the parameters of a realistic bending test of leaning standing tree such as most rubber trees in plantations (especially as they grow older that the example presented here). First, it was brought out that the computation of the bending moment applied by the wind can only be performed with the knowledge of the velocity profile of the wind, the height of the tree and its crown architecture (Petty and Swain, 1985; Peltola, 2006; Dellus *et al.*, 2004). In that way, the use of photographs, drawings, or any other representation of the crown can be a very good basis that can be coupled with a mechanical modelling to estimate the drag force and the resulting bending moment. This method is not standard in forest trees, because it is almost impossible to visualize non-destructively the front view of the crown in dense canopies; but it is usual for the assessment of wind firmness of urban trees in city parks (Dellus *et al.*, 2004).

It should be noted that the shape of the velocity profile of the wind (logarithmic, exponential...) could only be precisely determined by installing a mast equipped with several anemometers through its height. As an alternative method, a theoretical wind profile can be used; but for that we still need to calibrate them for rubber tree plantations.

Second, the impact of the drag force on the mechanical behaviour of the trunk requires the knowledge of the dimensions of the trunk and its mechanical properties. For example, the computation of the bending rigidity requires a correct description of the diameter variations along the height of the trunk. The intrinsic mechanical behaviour of the trunk can be assessed by performing bending tests on standing trees: The force applied is controlled, while the resulting longitudinal strains can be measured at different heights using strain sensors. This measurement makes possible to consider a possible variation of the local Young's modulus. To be perfectly precise, the rotation of the root anchorage and the evolution of the angle of the cable should also be taken into account during the bending tests in order to adjust the estimation of the bending moment.

In addition to the cable angle, it is necessary to measure and take into account the rotation of the root plate, as well as the elasticity and resulting shortening of the rope during the pulling test. Indeed, the displacement of the point of force application $v(z_F)$ (which can be assimilated to the deflection in a 3-points or 4-points bending test), corrected by the effect of root rotation, is related to the shortening ΔL according to equations 11 and 12. The knowledge of this displacement allows the estimation of the overall stiffness of the tree trunk. The application of the stem bending model with consideration of the tree crown weight showed that the impact of the weight should not be systematically neglected in the calculation of the total bending moment, especially in case of tilted trees. As the force applied during

the test increases, the relative effect of the crown weight becomes more and more important. This confirms the result of (Langbour, 1989; Moore et Gardiner, 2001), who also showed that the effect of weight was not always negligible. This point could be critical in case of strong bending tests that can be performed until the breakage of the trunk. And of course, it becomes non-negligible to estimate the bending moment on a tree submitted to high wind drag. In order to deduce a safety factor from these measurements, a growth stress assessment should be performed on the standing tree or after tree failure.

Conclusion and prospects

We developed a mechanical theoretical model that helps to analyse the bending test experiments on standing trees. This method was applied to a small test case provided by a preliminary experiment made on 2 rubber tree clones in a plantation in Ivory Coast. This test case is insufficient to provide statistically robust results, and was only provided here to illustrate the feasibility of our method and the insights that it may provide. It confirmed that our approach is comprehensive and feasible.

On this small test case, the analysis showed that the mechanical behaviour during the bending tests of the two clones appeared to be similar at the tree scale. For the estimate of the upper-bound drag force applied by the wind, the two clones showed contrasted behaviour with PB235 that showed a 70% higher drag force than the GT1 clone. This result is due to the large difference of architecture between the two clones.

Altogether, surprisingly, the computations indicate that the two clones seemed to display a rather high safety factor against a 12-grade wind storm, which does not seem to be consistent with wind damage records. This probably comes from the fact that bending tests and crown estimations were made on different plots and that we lack replications in this preliminary test case. However, even in these conditions, a clear clonal ranking could be achieved, with the GT1 trees in our small sample displaying a twice higher safety factor for wind firmness than PB235. This ranking is consistent with wind firmness reputation from wind damage historical records in African plantations.

In order to complete the analysis, we developed a simple model, not requiring complex theoretical calculations, that considers the weight of the crown and the resulting additional bending moment that is applied to the trunk during the test. The results showed that the relative impact of the crown is not negligible and increases with the height. Its estimation requires complementary data that are often missing in the experimental tests conducted so far (even in forest trees). But we now provide a straightforward method to conduct and analyse these tests and to provide the Rubber industry with clear quantitative data on clonal ranking for wind firmness at the adult stage.

Acknowledgments
The authors thank André Clément-Demange (CIRAD), Michel Gnagne (CNRA), Hyacinthe Legnaté (CNRA), and Dr Alexia Stokes (INRAE) for their contributions to the field mechanical experiments.

Funding and acknowledgements
This research on wind damage affecting cultivated rubber tree clones in plantations was funded by IFC (Institut Français du Caoutchouc) and its member-companies Michelin, SIPH and Socfin. Rubber tree data used in this study were collected from a previous interorganizational thematic research project ATP 97/60 funded by CIRAD, in partnership with CNRA (Centre National de Recherches Agronomiques de Côte d'Ivoire, Bimbresso research center), Ivory Coast.

Access to data
The data obtained during an experimental campaign in Côte d'Ivoire, in the experimental part of the Anguededou rubber plantation, are summarized in table I. The detailed measurements and analysis are available in the "Data INRAE Portail" with the following reference: Badel, Éric, 2022, "Tree bending tests", https://doi.org/10.15454/4BQ0LW.

References

Alméras T., Fournier M., 2009. Biomechanical design and long-term stability of trees: Morphological and wood traits involved in the balance between weight increase and the gravitropic reaction. Journal of Theoretical Biology, 256: 370-381. https://doi.org/10.1016/j.jtbi.2008.10.011

Ancelin P., Courbaud B., Fourcaud T., 2004. Development of an individual tree-based mechanical model to predict wind damage within forest stands. Forest Ecology and Management, 203: 101-121. https://doi.org/10.1016/j.foreco.2004.07.067

Blackburn G. R. A., 1997. The growth and mechanical response of trees to wind loading. Ph. D Thesis. University of Manchester, United Kingdom, 216 p. https://ethos.bl.uk/OrderDetails.do?uin=uk.bl.ethos.506075

Bossu J., Lehnebach R., Corn S., Regazzi A., Beauchêne J., Clair B., 2018. Interlocked grain and density patterns in *Bagassa guianensis*: changes with ontogeny and mechanical consequences for trees. Trees, 32: 1643-1655. https://doi.org/10.1007/s00468-018-1740-x

Brudi E., van Wassenaer P., 2002. Trees and statics: Non-destructive failure analysis. In: Tree Structure and Mechanics Conference Proceedings: How Trees Stand Up and Fall Down. Champaign, Ill, USA, International Society of Arboriculture, 17 p. https://www.tree-consult.org/upload/mediapool/pdf/baumstatik_und_biomechanik/trees-and-statics-nondestructive-failure-analysis.pdf

Cilas C., Costes E., Milet J., Legnaté H., Gnagne M., Clément-Demange A., 2004. Characterization of branching in two *Hevea brasiliensis* clones. Journal of Experimental Botany, 55: 1045-1051. https://doi.org/10.1093/jxb/erh114

CIRAD, 1990. L'hévéa. Bois et Forêts des Tropiques, 223 : 57-68. https://revues.cirad.fr/index.php/BFT/article/view/19680

Clément-Demange A., Chapuset T., Legnaté H., Costes E., Doumbia A., Obouayeba S., *et al.*, 1995. Wind damage: the possibilities of an integrated research for improving the prevention of risks and the resistance of clones in the rubber tree. In: Symposium on physiological and molecular aspects of the breeding of *Hevea brasiliensis*. IRRDB symposium, 1995-11-06/1995-11-07, Penang (Malaysia). Brickendonbury, UK, IRRDB, 182-199. http://agritrop.cirad.fr/464410

Clément-Demange A., Priyadarshan P. M., Tran Thy Tuy Hoa, Venkatachalam P., 2007. Hevea rubber breeding and genetics. Plant Breeding Reviews, 29: 177-283. https://doi.org/10.1002/9780470168035.ch4

Combe J.-Cl., du Plessix C.-J., 1974. Étude du développement morphologique de la couronne d'*Hevea brasiliensis* (Müll. Arg. Euphorbiacées-Crotonoïdées). Annals of Forest Science, 31 : 207-228. https://doi.org/10.1051/forest/19740402

Compagnon P., 1986. Le caoutchouc naturel : biologie, culture, production. Paris, France, Maisonneuve et Larose, 595 p. https://agritrop.cirad.fr/385180/

Cook N., 2007. Eurocode 1: Actions on structures - Part 1-4: General actions - Wind actions. London, UK, Thomas Telford Publishing, 124 p. https://www.boutique.afnor.org/en-gb/standard/nf-en-199114/eurocode-1-actions-on-structures-part-14-gereral-actions-wind-actions/fa104153/25897

Dellus V., Lesnino G., Wessoly L., 2004. Test de traction, premières applications en France. PHM - Revue Horticole, 461.

Donaldson L. A., Singh A. P., 2016. Chapter 6 - Reaction Wood. In: Secondary Xylem Biology. Elsevier, 93-110. https://doi.org/10.1016/B978-0-12-802185-9.00006-1

Fourcaud T., Clément-Demange A., Costes E., Baillères H., Gnagne M., 1999. Étude de la casse au vent chez l'hévéa : influence du modèle architectural. Compte rendu d'activité d'ATP Cirad, 60 : 16.

Fourcaud T., Clément-Demange A., Costes E., Gnagne M., 1998. Description of a simulation approach to investigate wind damage in rubber trees (*Hevea brasiliensis*). IUFRO Conference on Wind and Other Abiotic Risks to Forests, 1998, Helsinki, Finland.

Fournier M., Dlouhá J., Jaouen G., Almeras T., 2013. Integrative biomechanics for tree ecology: beyond wood density and strength. Journal of Experimental Botany, 64: 4793-4815. https://doi.org/10.1093/jxb/ert279

Gardiner B., Berry P., Moulia B., 2016. Review: Wind impacts on plant growth, mechanics and damage. Plant Science, 245: 94-118. https://doi.org/10.1016/j.plantsci.2016.01.006

Gohet E., Prévôt J.-C., Eschbach J.-M., Clément A., Jacob J.-L., 1996. Hevea latex production, relationship with tree growth, influence of clonal origin and Ethrel stimulation. In: Symposium on physiological and molecular aspects of the breeding of *Hevea brasiliensis*. IRRDB symposium, 1995-11-06/1995-11-07, Penang (Malaysia). Brickendonbury, UK, IRRDB, 200-216. https://agritrop.cirad.fr/464404

Gril J., Jullien D., Bardet S., Yamamoto H., 2017. Tree growth stress and related problems. Journal of Wood Science, 63: 411-432. https://doi.org/10.1007/s10086-017-1639-y

Hofmann J. P., 1984. Étude morphogénétique de la couronne de clones d'*Hevea brasiliensis* résistant et sensible à la casse au vent. Annals of Forest Science, 41 : 87-102. https://doi.org/10.1051/forest:19840106

Langbour P., 1989. Rigidité de l'arbre sur pied, indicateur de l'élasticité longitudinale du bois : application aux peupliers. Thèse de doctorat, science du bois, Institut national polytechnique de Lorraine, France, 196 p. https://agritrop.cirad.fr/594158/

Liu M., Vecchi G. A., Smith J. A., Knutson T. R., 2019. Causes of large projected increases in hurricane precipitation rates with global warming. npj Climate and Atmospheric Science, 2: 38. https://doi.org/10.1038/s41612-019-0095-3

Masson A., Monteuuis O., 2017. Plantations clonales d'hévéas issues de greffes ou de boutures. Bois et Forêts des Tropiques, 332 : 57-68. https://doi.org/10.19182/bft2017.332.a31333

Milet J., 2001. Analyse de l'architecture et comparaison de deux clones d'hévéa (*Hevea brasiliensis*) GT1-PB235. Mémoire de DESS, Université Montpellier 2, France, 108 p. https://agritrop.cirad.fr/484430/

Moore J., Gardiner B., 2001. Relative windfirmness of New Zealand-grown *Pinus radiata* and Douglas-fir: a preliminary investigation. New Zealand Journal of Forestry Science, 31: 208-223. https://www.scionresearch.com/__data/assets/pdf_file/0004/59332/Reprint-2769.pdf

Moore J., Gardiner B., Blackburn G. R., Brickman A., Maguire D. A., 2005. An inexpensive instrument to measure the dynamic response of standing trees to wind loading. Agricultural and Forest Meteorology, 132: 78-83. https://doi.org/10.1016/j.agrformet.2005.07.007

Nicolas D., 1979. Comportement de quelques clones d'hévea *Hevea brasiliensis* dans le Sud-est de la Côte d'Ivoire. Revue Générale du Caoutchouc et des Plastiques, 56 (593) : 175-181. https://agritrop.cirad.fr/426839/

Obouayeba S., Soumahin E. F., Okoma K. M., N'Guessan A. E. B., Coulibaly L. F., Koffi Kouablan E., *et al.*, 2012. Temporal and structural relations within bark and trunk in *Hevea brasiliensis* Muell. Arg. (Euphorbiaceae): Physiological maturity index of bark and latex vessels. International Journal of Biosciences, 2 (2): 56-71. https://agritrop.cirad.fr/565253/

Papesch A. J. G., Moore J. R., Hawke A. E., 1997. Mechanical stability of *Pinus radiata* trees at Eyrewell Forest investigated using static tests. New Zealand Journal of Forestry Science, 27: 188-204. https://www.scionresearch.com/__data/assets/pdf_file/0020/59510/NZJFS2721997PAPESCH188-204.pdf

Peltola H. M., 2006. Mechanical stability of trees under static loads. American Journal of Botany, 93: 1501-1511. https://doi.org/10.3732/ajb.93.10.1501

Petty J., Swain C., 1985. Factors influencing stem breakage of conifers in high winds. Forestry, 58: 75-84. https://doi.org/10.1093/forestry/58.1.75

Scurfield G., 1973. Reaction Wood: Its Structure and Function: Lignification may generate the force active in restoring the trunks of leaning trees to the vertical. Science, 179: 647-655. https://doi.org/10.1126/science.179.4074.647

Sellier D., Fourcaud T., 2005. A mechanical analysis of the relationship between free oscillations of *Pinus pinaster* Ait. saplings and their aerial architecture. Journal of Experimental Botany, 56: 1563-1573. https://doi.org/10.1093/jxb/eri151

Sellier D., Fourcaud T., 2009. Crown structure and wood properties: influence on tree sway and response to high winds. American Journal of Botany, 96: 885-896. https://doi.org/10.3732/ajb.0800226

Silpi U., Thaler P., Kasemsap P., Lacointe A., Chantuma A., Adam B., Gohet E., *et al.*, 2006. Effect of tapping activity on the dynamics of radial growth of *Hevea brasiliensis* trees. Tree Physiology, 26: 1579-1587. https://doi.org/10.1093/treephys/26.12.1579

Vecchi G. A., Delworth T. L., Murakami H., Underwood S. D., Wittenberg A. T., Zeng F., *et al.*, 2019. Tropical cyclone sensitivities to CO_2 doubling: roles of atmospheric resolution, synoptic variability and background climate changes. Climate Dynamics, 53: 5999-6033. https://doi.org/10.1007/s00382-019-04913-y

Wang J., Chen X., Cao L., An F., Chen B., Xue L., *et al.*, 2019. Individual Rubber Tree Segmentation Based on Ground-Based LiDAR Data and Faster R-CNN of Deep Learning. Forests, 10: 793. https://doi.org/10.3390/f10090793

Watson G. A., 1989. 4. Climate and soil. In: Webster C. C., Baulkwill W. J. (eds). Rubber. Harlow, UK, Longman Scientific and Technical, 125-164.

Yang M., Défossez P., Danjon F., Dupont S., Fourcaud T., 2017. Which root architectural elements contribute the best to anchorage of *Pinus* species? Insights from *in silico* experiments. Plant and Soil, 411: 275-291. https://doi.org/10.1007/s11104-016-2992-0

Engonga Edzang *et al.* – Author's contributions

Contributor role	Contributor names
Conceptualization	B. Moulia, E. Badel
Formal Analysis	J. Gril, E. Badel
Funding Acquisition	B. Moulia, E. Badel, T. Fourcaud
Investigation	A. C. Engonga Edzang, B. Niez, L. Heim, T. Fourcaud, E. Badel, J. Gril
Methodology	T. Fourcaud, E. Badel, J. Gril
Project Administration	E. Badel
Resources	T. Fourcaud
Supervision	E. Badel
Visualization	A. C. Engonga Edzang, E. Badel, J. Gril, B. Niez
Writing – Original Draft Preparation	A. C. Engonga Edzang, B. Niez, L. Heim
Writing – Review & Editing	E. Badel, J. Gril, B.Niez, B. Moulia, T. Fourcaud

Bois et Forêts des Tropiques - Revue scientifique du Cirad -
© Bois et Forêts des Tropiques © Cirad

Cirad - Campus international de Baillarguet,
34398 Montpellier Cedex 5, France
Contact : bft@cirad.fr - ISSN : L-0006-579X